

Synthesis and Transformation of Vanadyl Ethylene Glycolate, and Their Applications in a Lithium-Ion Battery

Qianwen Li¹, Yongchun Zhu¹, Yang Yu¹ and Yitai Qian^{1,2,*}

¹ Hefei National Laboratory for Physical Science at Microscale and Department of Chemistry, University of Science and Technology of China, Hefei, Anhui 230026, PR China

² School of Chemistry and Chemical Engineering, Shandong University, Jinan 250100, PR China

*E-mail: ytqian@ustc.edu.cn

Received: 15 April 2012 / Accepted: 21 May 2012 / Published: 1 June 2012

Vanadyl ethylene glycolate (VEG) spheres with an average diameter of $\sim 4\mu\text{m}$ composed of nanocubes were solvothermally prepared at 180 °C. The influence of temperature on the synthesis of VEG was investigated. When the temperature rised to 250 °C, the products experienced the transformation from VEG (IV) spheres to $(\text{NH}_4)_2\text{V}_6\text{O}_{16}(\text{V})$ flowers composed of flakes. Annealing the VEG (IV) spheres and $(\text{NH}_4)_2\text{V}_6\text{O}_{16}(\text{V})$ flakes in Ar atmosphere at 600 °C, V_2O_3 spheres and flakes were obtained. The electrochemical properties of the VEG and V_2O_3 were investigated in lithium-ion batteries. At a current density of 60 mA g⁻¹ the initial specific discharge capacity of VEG spheres was 1826 mAh g⁻¹ and even after 200 cycles the discharge capacity was still maintained at 477 mAh g⁻¹. The initial specific discharge capacities of V_2O_3 spheres and flakes were up to 1179 and 1338 mAh g⁻¹, respectively. After 50 cycles the discharge capacities of V_2O_3 spheres and flakes can also maintain at 466 and 665 mAh g⁻¹, respectively.

Keywords: vanadyl ethylene glycolate, transformation, V_2O_3 , electrochemical properties

1. INTRODUCTION

Due to the advantages of low cost, high abundance, easy synthesis and high energy density, the search for different kinds of vanadium oxides, VO_x (e.g. V_2O_5 , V_2O_4 , V_2O_3 , VO_2 , V_6O_{13}), have been studied for close to 40 years as possible materials for lithium-ion batteries (LIB) [1-5]. However, the vanadium oxides in LIB application are still limited by declining capacity and cyclic stability duo to irreversible phase transformation or even amorphization [6].

Thus, during the past decades, many efforts have been made to regulate the desired structure and morphology of vanadium oxides to improve the capacity retention [7-13]. The hydrothermal or

solvothermal method has been employed to synthesize various vanadium oxides with different structure and morphology. For example, yolk-shell V_2O_5 microspheres were synthesized via solvothermal route and subsequent calcination, which showed a capacity of 220 mAh g^{-1} after 30 cycles [14]. $(NH_4)_{0.5}V_2O_5$ nanobelts were hydrothermally synthesized, which showed a discharge capacity of about 141 mAhg^{-1} remaining after 100 cycles at a current density of 150 mA g^{-1} [15]. $VO_2(B)$ hollow microsphere were synthesized by annealing the nanothorn $VO_2(B)$ precursor hydrothermally prepared, which exhibited 200 mAhg^{-1} capacity retention after 50 cycles with a current density of 50 mA g^{-1} [16]. The hollow-dandelion VOOH hydrothermally prepared retained 120.6 mAhg^{-1} after 50 cycles at a current density of 100 mA g^{-1} [17]. Flowerlike V_2O_3 was solvothermally fabricated whose reversible discharge capacity was up to 200 mA g^{-1} after 30 cycles at a current density of 200 mA g^{-1} [18]. Lamellar V_2O_3 -based hybrid nanorods solvothermally prepared, which delivered a capacity up to 77 mAh g^{-1} after 50 cycles at a current density of 60 mA g^{-1} in aqueous lithium-ion battery [19]. Vanadyl ethylene glycolate (VEG) is always used as precursor to prepare other vanadium oxides [20, 21], while few researches about VEG itself were studied.

In this study, Vanadyl ethylene glycolate (VEG) composed of nanocube-based spherical microstructure with an average diameter of $\sim 4 \mu\text{m}$ was solvothermally prepared at $180 \text{ }^\circ\text{C}$. The influence of temperature on the synthesis of VEG in solvothermal process was investigated. When the temperature rised to $250 \text{ }^\circ\text{C}$, the products transformed from VEG (IV) spheres to $(NH_4)_2V_6O_{16}(V)$ flakes. Annealing the VEG (IV) spheres and $(NH_4)_2V_6O_{16}(V)$ flakes, V_2O_3 spheres and flakes were obtained. The properties of the VEG and V_2O_3 in rechargeable lithium batteries were investigated. At a current density of 60 mA g^{-1} the initial specific discharge capacity of VEG spheres is 1826 mAh g^{-1} and even after 200 cycles the discharge capacity is still maintained at 477 mAh g^{-1} . The initial specific discharge capacities of V_2O_3 spheres and flakes are up to 1179 and 1338 mAh g^{-1} . After 50 cycles the discharge capacities of V_2O_3 spheres and flakes can also maintain at 466 and 665 mAh g^{-1} , respectively.

2. EXPERIMENTAL DETAILS

2.1 Synthesis of the samples

All the reagents were of analytical grade and were used without any further purification. In a typical experiment, 0.234 g NH_4VO_3 were dissolved in 40 mL $C_2H_4O_2$ with stirring and formed a homogeneous solution. Then the solution was transferred into a Teflon-lined autoclave with a stainless steel shell. The autoclave was sealed and maintained at 180 , 200 , 220 , $250 \text{ }^\circ\text{C}$ for 24 h and then allowed to cool to room temperature naturally. The precipitate were collected and washed with distilled water and absolute ethanol. The obtained sample 1 ~ 4 were dried in a vacuum at $45 \text{ }^\circ\text{C}$ for 10 h . The sample A and B were obtained by putting the sample 1 ($180 \text{ }^\circ\text{C}$) and 4 ($250 \text{ }^\circ\text{C}$) into a porcelain boat with further heating at $600 \text{ }^\circ\text{C}$ for 3 h at a heating rate of $5 \text{ }^\circ\text{C}/\text{min}$ in a flowing Ar atmosphere with $5\% \text{ H}_2$ and then cooling to room temperature naturally.

2.2 Materials Characterization

The obtained products were characterized by X-ray diffraction (XRD) on a Philips X' pert with Cu K α radiation ($\lambda = 1.541874\text{\AA}$). The morphologies of the synthesized products were characterized on a Zeiss Supra 40 scanning electron microscope (SEM). XPS spectra of the products were obtained using an ESCALAB MK II spectrometer.

2.3 Electrochemical measurements

The electrochemical performances of the synthesized materials were evaluated in model CR2016 coin cells. The paste consisted of the positive active material prepared above, super P carbon black and polyvinylidene fluoride (PVDF) binder in a weight ratio of 75:15:10. The positive electrode was prepared by coating the paste on Al collector. Lithium foil was served as the negative and reference electrodes. The separator was Celgard 2320 membrane and the electrolyte was 1M LiPF₆ in ethylene carbonate (EC) and dimethyl carbonate (DMC) in volume ratio of 1:1. The cyclic tests and the open circuit voltage (OCV) data measurements were performed by Land automatic battery tester (Wuhan, China).

3.RESULTS AND DISCUSSION

A typical XRD pattern of the sample 1(180 °C) in Figure 1 could be readily indexed to monoclinic phase vanadyl ethylene glycolate (VEG, JCPDS no.49-2497). No peaks of other impurities were detected. Correspondingly, in Figure 2a and b, the SEM images reveal that VEG spheres with an average diameter of $\sim 4\mu\text{m}$ composed of nanocubes and little nanorods and the average size of nanocubes is about $\sim 400\text{ nm}$.

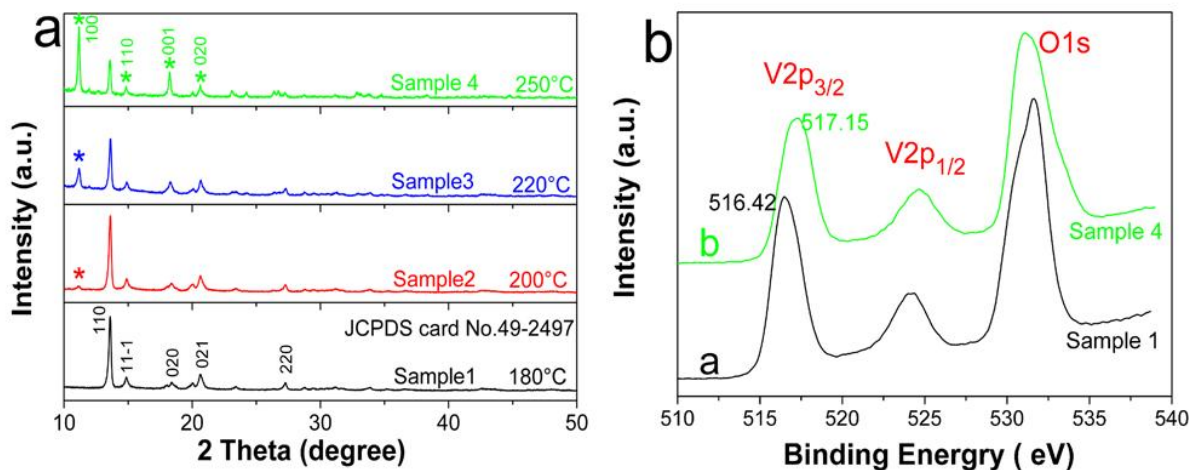


Figure 1. (a) The XRD patterns of the samples at 180, 200, 220, 250 °C (b) The XPS of the samples at 180, 250 °C

Further on, the influence of temperature on the synthesis of VEG in solvothermal process was investigated. When the temperature rises to 200 °C, the peak at 11.16° (labeled with *) appears which can not be observed in sample 1 (180 °C), but the intensity of this peak is very weak. With the temperature increasing to 220 °C, the intensity of the peak of 11.16° increases compared with the sample 2 (200 °C). When the temperature goes up to 250 °C, although the peak of (110) of VEG still exists, the intensity of the peak of 11.16° increases sharply, which is much stronger than the strongest peak of (110) of VEG. By analyzing data, the peak of 11.16° is the characteristic peak of (100) of monoclinic phase $(\text{NH}_4)_2\text{V}_6\text{O}_{16}$ (JCPDS no. 79-2051). With the sharp reduction of the intensity of (110) of VEG, the intensity of $(11\bar{1},1)$, (020) and (021) of VEG should descend correspondingly. However, in XRD patterns of sample 4, these peaks do not have the strong decrease. The reason may be that the other characteristic peaks of (110), (001) and (020) (labeled with *) of $(\text{NH}_4)_2\text{V}_6\text{O}_{16}$ coincide with the peaks of $(11\bar{1},1)$, (020) and (021) of VEG, respectively.

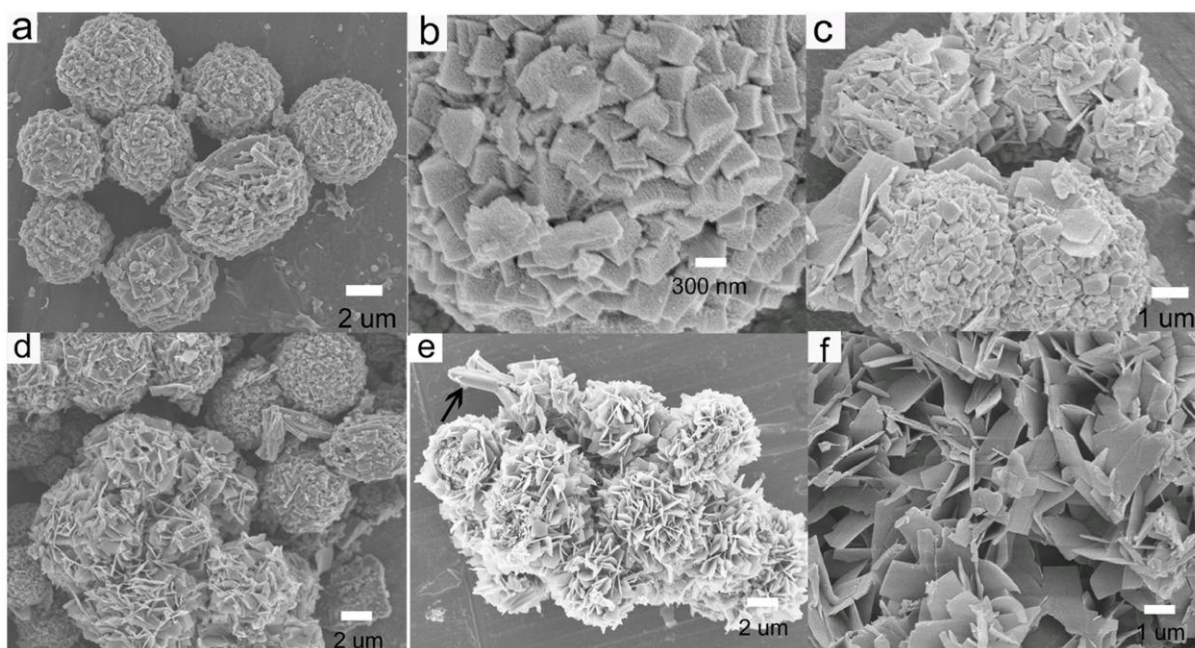


Figure 2. The SEM images of samples under different temperature (a,b) 180 °C (c) 200 °C (d) 220 °C (e,f) 250 °C

With the rise of the temperature, the typical SEM images of the samples at 200, 220, 250 °C were also presented in Figure 2. When the temperature rises to 200 °C, a very little flake microstructures uniting with the spheres by insertion were found in Figure 2c. With temperature increasing to 220 °C, much more flake microstructures can be observed in Figure 2d. As shown in Figure 2e, when the temperature is up to 250 °C, the main products were flowerlike microstructures composed of nanoflakes except for little small amounts of nanorod microstructures (marked by arrow). As a result, when temperature rises from 180 to 250 °C, the products experience the transformation from VEG (IV) spheres to $(\text{NH}_4)_2\text{V}_6\text{O}_{16}$ (V) flakes.

Also to ascertain the oxidation state of vanadium, the XPS spectra of the V 2p and O 1s regions of sample 1 (180 °C) and 4 (250 °C) are shown in Figure 1b. The binding energies of V 2p_{3/2} and V 2p_{1/2} in VEG are found to be 516.42 and 524.22 eV, respectively (Curve a). These values are the characteristic for vanadium (IV). When the temperature rises to 250 °C, as shown in Curve b the binding energy is shifted to higher position (V 2p_{3/2}, 517.15 eV; V 2p_{1/2}, 524.65 eV) indicating the formation of (NH₄)₂V₆O₁₆ where vanadium exists in +5. These values are identical with the reported literature [22]. It is believed that the temperature has an important influence on the valence and morphology of vanadium oxides in solvothermal process.

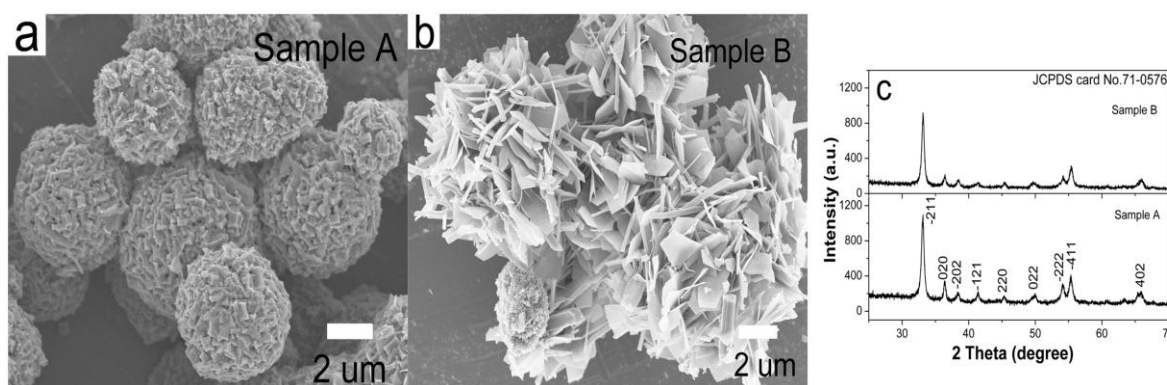


Figure 3. (a,b)The SEM images of sample A and B (c)The XRD patterns of Sample A and B

Annealing the as-prepared products sample 1 (180 °C) and sample 4 (250 °C) in Ar atmosphere with 5% H₂, Sample A and B were obtained. It is worth noting that the perfect inheritance of the morphology of their precursors. The morphology of Sample A in Figure 3a presents that spherical microstructures with an average diameter of ~ 4 μm. The morphology of Sample B in Figure 3b still appears the nanoflake microstructures. The XRD patterns of Sample A and B in Figure 3c could be readily indexed to be a monoclinic V₂O₃ (JCPDS card No. 71-0576).

Figure 4a shows voltage versus discharge capacity curves at the 1st, 2nd, 100th and 200th cycles for the VEG cell during 0.01-3V at a current density of 60 mA g⁻¹. It does not indicate a stable discharge plateau, which is similar as other vanadium oxides [17, 21]. The initial specific discharge capacity of VEG is 1826 mAh g⁻¹ and the second discharge capacity decays to 616 mAh g⁻¹. The discharge capacity has no obvious fading with the progress of the cycle. After the 100th cycle, the discharge capacity of 519 mAh g⁻¹ is still maintained. Even after 200 cycles the discharge capacity is still up to 477 mAh g⁻¹. The inset in Figure 4a shows the cyclic performance of the VEG electrode. The XRD patterns of the work material of VEG/Li cell after 1 cycle and 200 cycles are shown in Figure 4b. Only the peak of (110) of VEG can be observed. Figure 4c shows the morphology of the work material of VEG/Li cell after 1 cycle. The spherical microstructures disappeared and the aggregation of nanoparticles about ~1μm were observed. In Figure 4d after 200 cycles, these nanoparticles from VEG/Li cell is in better dispersion than the particles after 1 cycle.

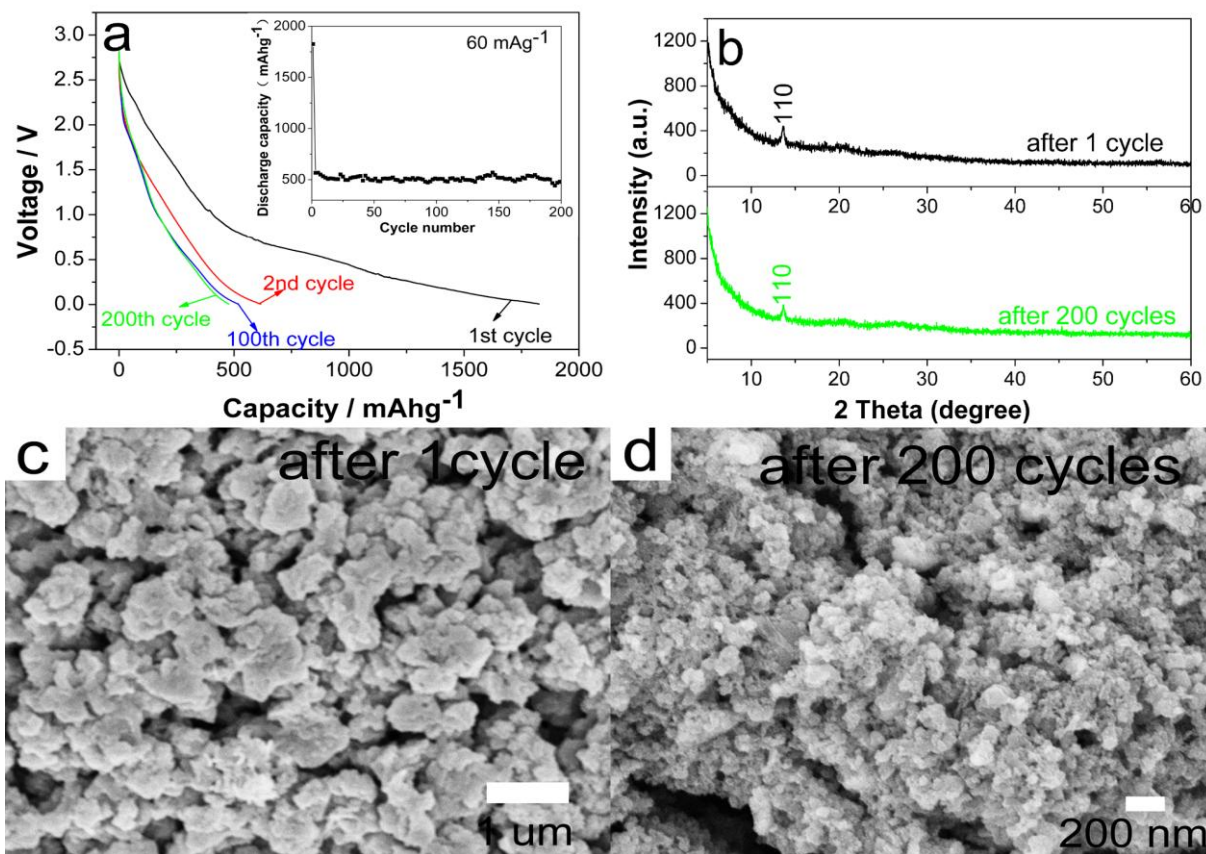


Figure 4. (a) Voltage versus discharge capacity curves at the cycling rate of 60 mA g^{-1} for the VEG/Li cell between 0.01 and 3V at the 1st, 2nd, 100th and 200th cycles. The insets shows the corresponding cyclic performance of the cell (b) the XRD patterns of the samples from VEG/Li cell after 1st cycle, 200th cycles (c,d) the SEM images of samples from VEG/Li cell after 1st cycle, 200th cycles

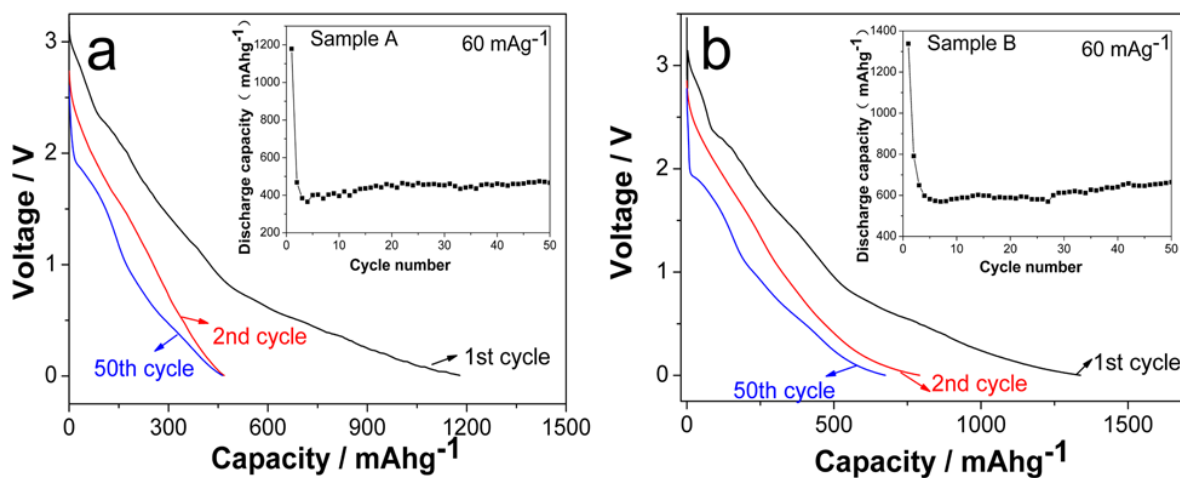


Figure 5. Electrochemical performances of $\text{V}_2\text{O}_3/\text{Li}$ cell: discharge capacity at the cycling rate of 60 mA g^{-1} between 0.01 and 3 V (a) V_2O_3 spheres (b) V_2O_3 flakes. The insets show voltage versus discharge capacity curves at the 1st, 2nd, and 50th cycle.

It gives a hint that the transformation of structure from the nanocube-based spheres to the aggregation of nanoparticles may bring in the irreversible capacity loss during first charge and discharge. During the later cycling, the structure of the work materials of VEG/Li cell has no distinct change. Correspondingly, the discharge capacity also has no obvious fading. The electrochemistry performances of V_2O_3 spheres and flakes were also studied in lithium-ion batteries. Figure 5a and b display the curves of voltage versus discharge capacity for V_2O_3 spheres and flakes cell between 0.01 and 3 V at a current density of 60 mAh g^{-1} for the 1st, 2nd, and 50th cycles. The initial specific discharge capacities of V_2O_3 spheres and flakes are 1179 and 1338 mAh g^{-1} , respectively. The second discharge capacities decay to 468 and 792 mAh g^{-1} . After the 50th cycle, the discharge capacities of V_2O_3 spheres and flakes are still maintained at 466 and 665 mAh g^{-1} . With increasing number of cycles, the capacities tend to fade slowly after the initial capacity loss. The reason may be the existence of an amorphous phase in the material [18]. The insets in Figure 5a and b show the cyclic performance of the spheres and flakes electrode, respectively. The V_2O_3 flakes show a better rate capability than V_2O_3 spheres. The uniform flake-like morphology may provide a high electrode/electrolyte contact area and speed up the intercalation and extraction processes [23, 24].

4. CONCLUSION

Vanadyl ethylene glycolate (VEG) composed of nanocube-based spherical microstructure with an average diameter of $\sim 4 \mu\text{m}$ was solvothermally prepared at $180 \text{ }^\circ\text{C}$. The influence of temperature on the synthesis of VEG were investigated. When the temperature rises to $250 \text{ }^\circ\text{C}$, the products experience the transformation from VEG (IV) spheres to $(\text{NH}_4)_2\text{V}_6\text{O}_{16}$ (V) flakes. Annealing the VEG (IV) spheres and $(\text{NH}_4)_2\text{V}_6\text{O}_{16}$ (V) flakes in Ar atmosphere at $600 \text{ }^\circ\text{C}$, V_2O_3 spheres and flakes were obtained. The electrochemical properties of the VEG and V_2O_3 were investigated. At a current density of 60 mA g^{-1} the initial specific discharge capacity of VEG spheres is 1826 mAh g^{-1} and even after 200 cycles the discharge capacity is still maintained at 477 mAh g^{-1} . The initial specific discharge capacities of V_2O_3 spheres and flakes are up to 1179 and 1338 mAh g^{-1} . After 50 cycles, the discharge capacities of V_2O_3 spheres and flakes can also maintain at 466 and 665 mAh g^{-1} , respectively. It is believed that the temperature has an important influence on the valence and morphology of vanadium oxides in solvothermal process. Meanwhile, the obtained nano/microstructured materials VEG and V_2O_3 through this method may be promising candidates to employ as electrode material in rechargeable lithium batteries. Much more work to get higher electrochemical performance is under progress.

ACKNOWLEDGEMENT

This work was financially supported by the National Nature Science Fund of China (No. 91022033) and the 973 Project of China (No. 2011CB935901).

References

1. D.W. Murphy, P.A. Christian, F.J. Disalvo and J.N. Carides, *J. Electrochem. Soc.*, 126 (1979) 497

2. M.A. Zoubi, H.K. Farag and F. Endres, *Journal of Materials Science*, 44 (2008) 1363
3. S.J. Zhuo, M.W. Shao, Q. Zhou and F. Liao, *Electrochim. Acta*, 56 (2011) 6453
4. H. Wang, K. Huang, S. Liu, C. Huang, W. Wang and Y. Ren, *J. Power Sources*, 196 (2011) 788
5. C. Wu and Y. Xie, *Energy Environ. Sci.*, 3 (2010) 1191
6. Y. Wang and G. Cao, *Adv. Mater.*, 20 (2008) 2251
7. A. Talledo and C.G. Granqvist, *J. Appl. Phys.*, 77 (1995) 4655
8. H.P. Wong, B.C. Dave, F. Leroux, J. Harreld and L.F. Nazar, *J. Mater. Chem.*, 8 (1998) 1019
9. L.J. Fu, H. Liu, C. Li, Y.P. Wu, E. Rahm and R. Holze *et al.*, *Prog. Mater Sci.*, 50 (2005) 881
10. H. Heli, H. Yadegari and A. Jabbari, *J. Phys. Chem. C*, 115 (2011) 10889
11. H. Liu and W. Yang, *Energy Environ. Sci.*, 4 (2011) 4000
12. S. Wang, S. Li, Y. Sun, X. Feng and C. Chen, *Energy Environ. Sci.*, 4 (2011) 2854
13. X. Liu, J. Wang, J. Zhang and S. Yang, *Journal of Materials Science*, 42 (2007) 867
14. J. Liu, Y. Zhou, J. Wang, Y. Pan and D. Xue, *Chem. Commun.*, 47 (2011) 10380
15. H. Wang, K. Huang, C. Huang, S. Liu, Y. Ren and X. Huang, *J. Power Sources*, 196 (2011) 5645
16. H. Liu, Y. Wang, K. Wang, E. Hosono and H. Zhou, *J. Mater. Chem.*, 19 (2009) 2835
17. C. Wu, Y. Xie, L. Lei, S. Hu and C. OuYang, *Adv. Mater.*, 18 (2006) 1727
18. H. Liu, Y. Wang, H. Li, W. Yang and H. Zhou, *ChemPhysChem*, 11 (2010) 3273
19. Y. Sun, S. Jiang, W. Bi, C. Wu and Y. Xie, *J. Power Sources*, 196 (2011) 8644
20. P. Ragupathy, S. Shivakumara and N. Munichandraiah, *J. Phys. Chem. C*, 112 (2008) 16700
21. Y. Xu, L. Zheng, C. Wu, F. Qi and Y. Xie, *Chem. Eur. J.*, 17 (2011) 384
22. R. Lindstrom, V. Maurice, H. Groult and C. Cohen *et al.*, *Electrochim. Acta*, 51 (2006) 5001
23. M. Zhang, Q. Chen, Z. Xi, Y. Hou and Q. Chen, *Journal of Materials Science*, 47 (2011) 2328
24. S. Zhang, Y. Li, C. Wu, F. Zheng and Y. Xie, *J. Phys. Chem. C*, 113 (2009) 15058